

## REVIEW

View Article Online  
View Journal | View Issue



Cite this: *Org. Biomol. Chem.*, 2020, **18**, 1697

## Insights into DNA catalysis from structural and functional studies of the 8-17 DNAzyme†

Marjorie Cepeda-Plaza \*<sup>a</sup> and Alessio Peracchi \*<sup>b</sup>

DNAzymes (deoxyribozymes) are single-stranded DNA molecules endowed with catalytic activity, obtained by *in vitro* selection. In the past 25 years, dozens of DNAzymes have been identified and employed for applicative purposes, yet our knowledge of the structural and mechanistic basis of DNA catalysis remains very limited. The RNA-cleaving 8-17 DNAzyme, which depends on divalent metal ions for function, is possibly the most studied catalytic DNA in terms of mechanism. It is very efficient, implying that it adopts a combination of distinct catalytic strategies, but until recently it was uncertain which strategies are at play and how they are implemented. Recently, however, new functional studies and the attainment of high-resolution X-ray structures of an 8-17 construct, have offered a great opportunity for a more detailed understanding of its mechanism. This review examines the functional information gathered on 8-17, in the light of the available crystal structures, pointing out the congruences and possible inconsistencies between the functional and structural data. We will analyze separately three aspects of the DNAzyme function: the structural requirements for catalysis, the role of metal ions and the influence of pH on activity. Ultimately, we will contrast the experimental data with a model for the 8-17 mechanism proposed in the crystallographic study, whereby one specific G residue (G14) acts as a general base and a metal-coordinated water molecule acts as a general acid. Throughout this analysis we will signal the most outstanding mechanistic issues that remain to be addressed, with implications for the broader field of DNA catalysis.

Received 13th November 2019,  
Accepted 28th January 2020

DOI: 10.1039/c9ob02453k

rscl.li/obc

## Introduction

In 1994 Breaker and Joyce reported the identification and characterization of the first DNAzyme (deoxyribozyme, catalytic DNA),<sup>1</sup> demonstrating that DNA can promote enzymatic functions.<sup>1–3</sup> DNAzymes are short single-stranded DNA molecules with catalytic properties obtained by a combinatorial process called *in vitro* selection.<sup>4,5</sup> Over the years, many different DNAzymes have been selected, capable of catalyzing a wide array of reactions, including RNA/DNA cleavage, RNA ligation, covalent modification of amino acid side chains, DNA depurination, and Diels–Alder reactions.<sup>6</sup> The remarkable features of DNAzymes such as great stability, relatively easy chemical modification and low cost, in addition to their versatility, efficient activity and flexibility in substrate recognition, make them excellent candidates for a variety of biotechnological and pharmaceutical applications. For example, RNA-cleaving DNAzymes

have been used extensively as selective metal-ion-based sensors for environmental, industrial and *in vivo* sensing.<sup>7,8</sup> Furthermore, important applications in downregulation of therapeutically relevant RNAs have been developed.<sup>9,10</sup> Despite all this applicative interest, information about the structures and precise mechanisms of these enzymes is still limited.

One of the best known RNA-cleaving DNAzymes is the 8-17 motif.<sup>3</sup> This catalytic DNA depends on divalent metal ions to function and variants of this motif have been repeatedly isolated during *in vitro* selection procedures, carried out independently by different groups.<sup>11–13</sup> The 8-17 has received much attention both in terms of mechanism and of applications<sup>14</sup> becoming a model system in the field of catalytic DNA. Over the last 22 years, the 8-17 DNAzyme has been the subject of numerous chemical, enzymological and biophysical studies, aimed at understanding the reaction mechanism and the structural basis of activity.

In 2017 Liu *et al.* reported the first three-dimensional structure of the 8-17 DNAzyme.<sup>15</sup> Crystals of 8-17 bound to an uncleavable substrate analog were grown in the presence of DNA polymerase X from African swine fever virus. The protein facilitated crystallization and molecular packing but formed only marginal interactions with the DNAzyme. Three crystal structures were solved – two in which the DNAzyme was bound

<sup>a</sup>Chemical Sciences Department, Universidad Andres Bello, Santiago, Chile.  
E-mail: marjorie.cepada@unab.cl

<sup>b</sup>Department of Chemistry, Life Sciences and Environmental Sustainability, University of Parma, Parma, Italy. E-mail: alessio.peracchi@unipr.it

†Electronic supplementary information (ESI) available. See DOI: 10.1039/c9ob02453k

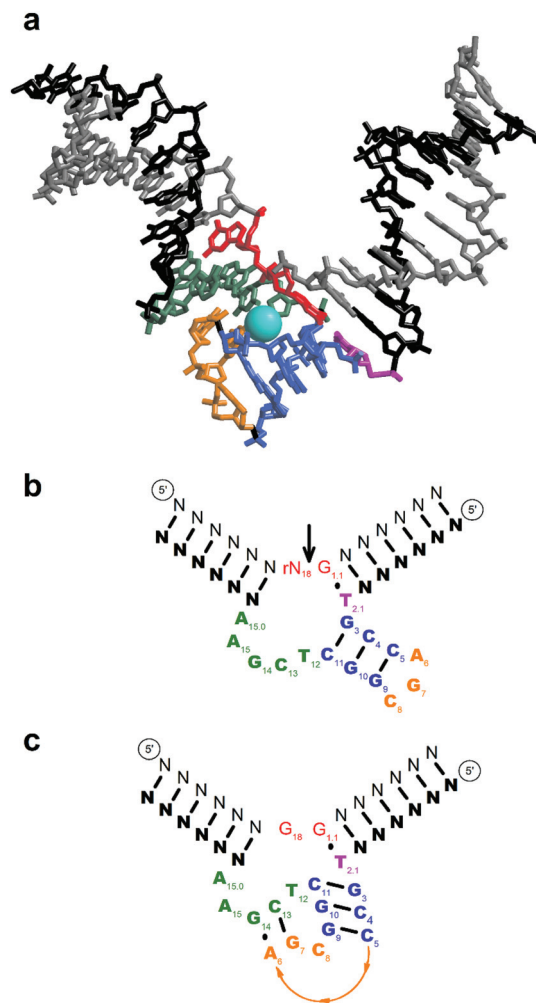


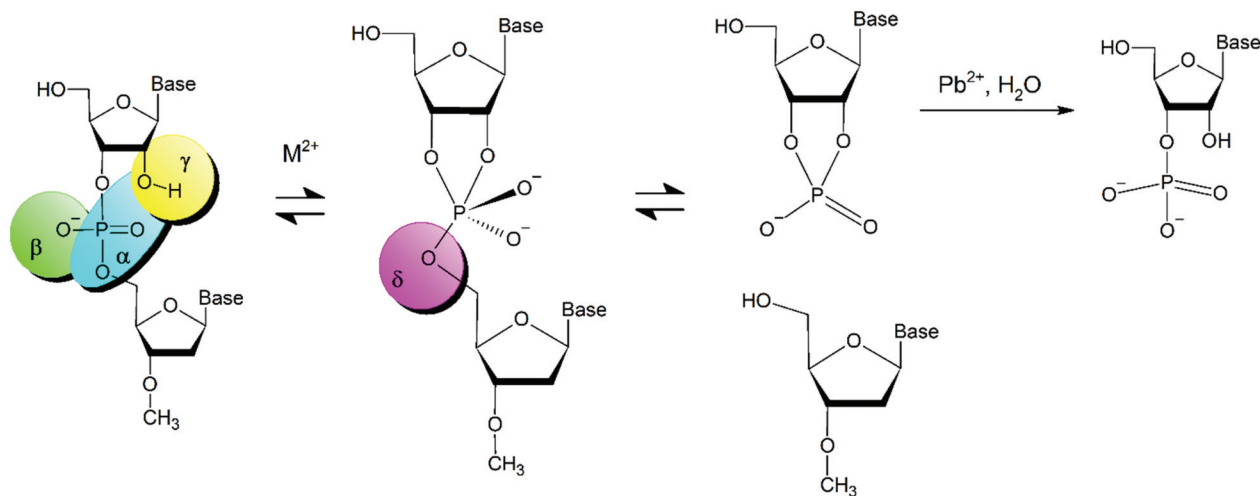
**Fig. 1** The 8-17 DNAzyme (a) overview of the three-dimensional structure of the DNAzyme, bound to an uncleavable substrate analog. This is a rendering of the structure solved by Liu *et al.* in the presence of  $\text{Pb}^{2+}$  (PDB code 5XM8).<sup>15</sup> The substrate binding arms are shown in black; the T2.1 residue (nucleotides are numbered according to Peracchi<sup>16</sup>) is in purple; the core stem in blue; the AGC loop in orange and the bulge loop in green. In the substrate strand (light gray) the two residues between which cleavage occurs are shown in red. The  $\text{Pb}^{2+}$  ion bound to the DNAzyme core is shown as a cyan sphere. (b) Conventional representation of the secondary structure, following the original work by Santoro and Joyce.<sup>3</sup> In the enzyme strand (bold letters) different regions are color-coded as in panel a. The cleavage site is indicated by an arrow. The residue at the cleavage site (rN18) can be any ribonucleotide, but conventional 8-17 constructs cleave most efficiently after purine residues (rA or rG).<sup>17</sup> Similarly, the following nucleotide is typically a G (G1.1), even though variants of the 8-17 that cleave quite efficiently substrates with an A or a C at this position have been isolated.<sup>18</sup> (c) Revised secondary structure representation, based on the specific construct used in the crystallographic study, showing in particular, the base-pairing of residues A6 and G7 with residues G14 and C13. Another unpredicted pairing between A15 and G18, observed in the crystal structure, is not shown both for clarity and because its functional significance remains uncertain (see main text). It should be noted that the residue numbering used here (and in most of the functional literature) differs from the numbering used in the structural paper,<sup>15</sup> which in turn differs from the numbering provided in the PDB file of the 8-17 structure. To help the reader, a table comparing the three numbering systems is provided in ESI Table 1.†

to an all-DNA substrate analog (one structure in the absence of divalent metal ions and the other in the presence of  $\text{Pb}^{2+}$ ) and a third structure obtained with a substrate analog bearing a 2'-*O*-methyl group at the cleavage site (in the absence of divalent metal ions). While the structure with  $\text{Pb}^{2+}$  bound showed the highest resolution at 2.55 Å, the organization of the core was remarkably constant in all three cases. Overall, the DNAzyme is V-shaped, with the two helical substrate-binding arms forming an angle of ~70 degrees and converging towards one twisted DNA pseudoknot (Fig. 1a).<sup>15</sup> Such a compacted pseudoknot, combined with a large cavity that accommodates  $\text{Pb}^{2+}$ , were perhaps the most surprising features of the crystal structure. They also appeared important to help explain several aspects of the 8-17's catalytic behavior, as it will be detailed below.

The aim of the present review article is to summarize and examine the most relevant functional studies carried out on the 8-17 DNAzyme in the past two decades, evaluating this information in the light of the recently reported crystal structure.<sup>15</sup> Here we will analyze separately (to the extent this is possible) three aspects of the DNAzyme function: the structural requirements for activity, the role of metal ions and the influence of pH on activity. Regarding each aspect, we will outline first what the functional studies had uncovered before attainment of the crystal structure; and then we will show how the crystal structure has illuminated and put in context the prior functional knowledge. This kind of organization should help appreciate not just our current understanding of the structure-mechanism relationships in the 8-17 DNAzyme, but also how this understanding has been built. We will discuss the congruences and possible discordances between the functional data and the reported structural features, pinpointing the most outstanding questions that remain to be addressed regarding the 8-17, with implications for the broader field of DNA catalysis.

## Chemical mechanism and possible catalytic strategies for the 8-17-catalyzed transesterification reaction

The RNA-cleaving reaction catalyzed by the 8-17 occurs through the internal nucleophilic attack of the 2'-oxygen of the ribose ring on the phosphodiester linkage, forming a penta-coordinated species (transition state or short-lived intermediate), which evolves to form a 2',3'-cyclic phosphate and a 5'-hydroxyl terminal RNA fragments in presence of metal ion cofactors such as  $\text{Mg}^{2+}$  and  $\text{Zn}^{2+}$ , while in presence of  $\text{Pb}^{2+}$  the DNAzyme catalyzes a two-step reaction mechanism in which the aforementioned transesterification reaction is followed by hydrolysis of the 2',3'-cyclic phosphate.<sup>17,19</sup> The general mechanism of the reaction is depicted in Scheme 1. The spontaneous cleavage of RNA (corresponding to the transesterification reaction in Scheme 1) occurs typically with a rate constant of  $\sim 10^{-8} \text{ min}^{-1}$  (at room temperature, neutral pH and in the



**Scheme 1** Mechanism of RNA cleavage by an internal phosphodiester transfer reaction. The four main strategies suggested for catalytic activation are denoted in Greek lettering as follow: in-line nucleophilic attack ( $\alpha$ , light blue), neutralization of the non-bridging phosphate oxygen ( $\beta$ , green), deprotonation of the 2'-OH group ( $\gamma$ , yellow) and stabilization of the 5'-O leaving group ( $\delta$ , pink).<sup>19</sup> When these strategies are mentioned in the text, they will be categorized as primary, secondary and tertiary according to each case.<sup>21</sup>

presence of 5 mM  $\text{Mg}^{2+}$ ).<sup>20</sup> Nucleic acid enzymes can accelerate this reaction by eight to ten orders of magnitude. Four catalytic strategies have been proposed in the reaction mechanism of RNA-cleavage by nucleic acid enzymes to explain the order of acceleration achieved: (i) in-line nucleophilic attack ( $\alpha$ -catalysis), (ii) neutralization of the non-bridging phosphate oxygen ( $\beta$ -catalysis), (iii) deprotonation of the 2'-hydroxyl group ( $\gamma$ -catalysis) and finally, (iv) stabilization of the 5'-oxygen leaving group ( $\delta$ -catalysis).<sup>19</sup> These strategies are highlighted in colors in Scheme 1. Very recently a new framework has been proposed to stratify these strategies as primary, secondary and tertiary according to the level of contribution of atoms or groups from the catalytic core in the chemical reaction. The  $\beta$ ,  $\gamma$  and  $\delta$  catalytic strategies can be categorized under this new terminology, however this latest classification is not applied for  $\alpha$  catalysis.<sup>21</sup>

The 8-17 DNAzyme is remarkably efficient, with an estimated maximum rate of  $220 \text{ min}^{-1}$ , under optimal conditions using  $\text{Pb}^{2+}$  as a cofactor.<sup>17</sup> This implies that the enzyme cleaves RNA by adopting a combination of distinct catalytic strategies,<sup>19</sup> however until recently it was not clear which strategies are actually at play in its mechanism, and by which means they are implemented. In the following sections we will examine our current understanding of the mechanism of the 8-17 DNAzyme, relating this information to the four strategies above and their level of contribution. In particular, towards the end of the review, we will discuss a first detailed model for the 8-17 catalytic mechanism, proposed in the crystallographic study,<sup>15</sup> in which a specific guanosine residue (G14) acts as a general base to abstract a proton from the 2'-OH (primary  $\gamma$  strategy) while a hydrated divalent metal ion is proposed to function as a general acid, protonating the 5'-hydroxyl leaving group (secondary  $\delta$ -catalysis). The features, limits and possible alternatives to such a model will be evaluated.

## What functional studies say about the 8-17's sequence and structural requirements for catalysis

An initial view of the secondary structure adopted by the deoxyribozyme complexed to its substrate was provided in the original study by Santoro and Joyce.<sup>3</sup> This view was subsequently enriched but not substantially altered by a number of other *in vitro* selection and mutational studies.<sup>11,13,16–18,22–25</sup> The conventional depiction of the secondary structure is shown in Fig. 1b, together with the residue numbering most often adopted in the functional literature. In the secondary structure, the DNAzyme hybridizes to its substrate *via* two 'arms' that can be changed in terms of length and sequence. In the substrate strand, the nucleotide at the cleavage site (A in the original study) is unpaired and typically followed by a G residue (G1.1).<sup>11</sup> The residue at the cleavage site needs to be a ribonucleotide (given the mechanism of cleavage adopted by the 8-17) whereas all other nucleotides in the substrate strand can be deoxyribonucleotides. As a matter of fact, even though the composition of the DNAzyme–substrate helices can be varied almost at will and also include unnatural nucleotides,<sup>3,26</sup> a mostly-DNA substrate is cleaved more efficiently than an all-RNA substrate.<sup>11,16</sup>

Since the earliest studies, it was clear that the cleavage activity of 8-17 relies on a small "core" of relatively conserved nucleotides in the catalytic strand, not involved in standard base pairing with the substrate.<sup>3</sup> The core encompasses a conserved T residue (T2.1) that faces G1.1, then a three-basepair intramolecular helix (the "core stem"), surmounted by an AGC loop (residues 6–8). The stem is followed by a short stretch of four or five nucleotides (residues 12 to 15 or 15.0, often referred to as the "bulge loop"), that were not predicted to participate in a standard secondary structure.

Within this core, the results of *in vitro* selections and mutational studies had allowed the identification of nucleotides strictly required for catalysis, providing also initial suggestions about their potential role. In particular:

(i) The study in which the 8-17 was first identified suggested that T2.1 could form a wobble pair with the facing, conserved G residue on the substrate strand.<sup>3</sup> The geometry, rather than the stability of this pair seemed important for catalysis. In fact, replacing T2.1 with any other standard nucleotide was functionally deleterious and in particular changing it to a C (which would allow formation of a standard GC pair) had a >1000 fold impact on catalysis.<sup>18,22</sup> Also, reversing the pair from G1.1-T2.1 to T1.1-G2.1 was incompatible with activity.<sup>17</sup>

(ii) The core stem had to be three bp long. Longer helices yielded catalytically inactive molecules.<sup>3</sup> Moreover, although constructs whose core stem contained mismatches or bulges were reported to show some activity,<sup>13</sup> catalytic efficiency seemed loosely correlated with the estimated stability of this short duplex.<sup>3,11,22</sup> The less-than-perfect relationship between predicted stability and activity had perhaps something to do with the core stem conformation: intriguingly, circular dichroism experiments suggested that the stem would adopt a Z-helix form, at least in the presence of metal ions different from Pb<sup>2+</sup>.<sup>23</sup> Some data also hinted that the central base pair of the stem might play a more specific functional role: in one construct, optimal activity seemed associated to a C4-G10 central basepair,<sup>22</sup> whereas in another construct the identity of the central pair affected the selectivity for different metal cofactors.<sup>27</sup>

(iii) The AGC loop appeared to be particularly important for function. The two purines in the loop were strictly required for activity. Substituting the A6 or G7 with non-standard nucleotides (such as 7-deazaA or thioG) suggested that the bases of these residues are involved in a close-contact interaction with some other part of the molecule – an interaction involving multiple hydrogen bonds.<sup>22</sup> In terms of catalysis, the strongest impacts were observed upon removing or replacing the N7 group from A6 or the 6-keto function from G7.<sup>22</sup> The involvement of A6 and G7 in a hydrogen bond network was supported by the results of a three-color single-molecule FRET study, whose authors proposed that interactions formed by residues A6 and G7 play a critical role in folding.<sup>28</sup> Leung and Sen, who studied the pattern of charge (electron hole) migration through the folded 8-17 DNAzyme–substrate complex, observed a rather low exposition of G7 to the solvent.<sup>29</sup>

(iv) In the “bulge loop”, *i.e.* the stretch of apparently unpaired nucleotides following the core stem, C13 and G14 were most crucial: replacement of either residue with other standard nucleotides invariably decreased catalysis by over three orders of magnitude.<sup>22</sup> The two residues were assumed to be most closely involved in catalysis,<sup>13</sup> but there was good evidence that C13 would not act as a general acid–base catalyst.<sup>22</sup> In addition, a photo-crosslinking study, investigating the proximity between different nucleotides and the cleavage site, suggested that G14 had to be particularly close to G1.1 and G18.<sup>30</sup> In contrast to the apparently central role of C13

and G14, the other nucleotides in this region were relatively tolerant of mutations and seemed to play ancillary functions.<sup>22</sup> They would at most affect the selectivity of the DNAzyme for different metal ion cofactors.<sup>16,22,31,32</sup> A15 apparently becomes less stacked upon the binding of activating metal ions.<sup>33</sup> A15.0 was dispensable: mutants in which this nucleotide was replaced by an abasic residue<sup>24</sup> or even removed altogether,<sup>3,17</sup> retained substantial activity; nevertheless in most cases the presence of A15.0 helped achieve a better catalytic efficiency.<sup>3,17,22</sup>

Despite the rich information gathered in all these functional studies, no detailed model structure was proposed for the DNAzyme core. From the examination of many selected 8-17 variants, Cruz and coworkers deduced a very crude structural model that distinguished between an inner group of residues most intimately involved in catalysis (in practice, C13, G14 and the two substrate nucleotides flanking the cleavage site, plus possibly a metal ion) and a ‘facilitator’ domain that included all other residues in the core.<sup>13</sup> Based on photo-cross-linking data, Liu and Sen put forward another rough model for the active conformation of the 8-17 DNAzyme;<sup>30</sup> such a model tentatively placed the cleavable phosphodiester between the A6G7 residues (from the AGC loop) on one side and the C13G14 couple on the opposite side.

## Comparing the functional data with the 8-17 three-dimensional structure

It was gratifying to observe that the recent crystal structure of 8-17<sup>15</sup> was consistent with the majority of the functional data – this is not always the case with small catalytic nucleic acids, since these molecules are prone to adopt different folds and hybridization patterns.<sup>34</sup> An instructive example comes from studies on the hammerhead ribozyme. When the first crystal structures of ‘minimal’ hammerhead constructs were solved,<sup>35,36</sup> the results were not fully compatible with the mutagenesis and functional studies, revealing several puzzling discrepancies.<sup>35–37</sup> To explain such discrepancies it was hypothesized that the crystal structure of the hammerhead reflected an inactive conformer, that needed to undergo some major conformational change to perform catalysis.<sup>38,39</sup> This prediction was confirmed by a subsequent crystallographic study on a more extended (and more active) hammerhead construct,<sup>40</sup> showing a core structure largely rearranged with respect to the initial structures and much more consistent with the functional data.<sup>41</sup>

In the case of the 8-17 DNAzyme, the structure confirmed the proximity to the cleavage site of the same conserved residues that were previously revealed by a variety of biochemical assays.<sup>15</sup>

(i) In the crystal structures, T2.1 forms indeed a wobble pair with G1.1, while also stacking on top of the core stem. As judged from the available structures, pairing of G1.1 with T2.1 seems potentially important for two reasons. First it helps stretching and positioning the phosphodiester bond at the



cleavage site, forming a 'kink' in the substrate strand and assisting an in-line arrangement that is a prerequisite for catalysis ( $\alpha$  strategy, Scheme 1). Second, it may help define a cavity where the  $\text{Pb}^{2+}$  ion can be accommodated.

(ii) The three-bp core stem is there as predicted (Fig. 1c) and is identified as P3 in the crystallographic paper. It adopts a right-handed helical geometry. T2.1 stacks on one end of the helix, while C8 (from the AGC loop) stacks on the other end. The limited length and the geometry of the core stem apparently helps the interaction of the other two residues of the AGC loop (G7 and A6) with C13 and G14 in the bulge loop (Fig. 2; see below). Furthermore, the stem provides a 'wall' on one side of the cavity where  $\text{Pb}^{2+}$  is observed to bind, and the central pair is roughly co-planar with the metal ion (Fig. 1a).<sup>15</sup>

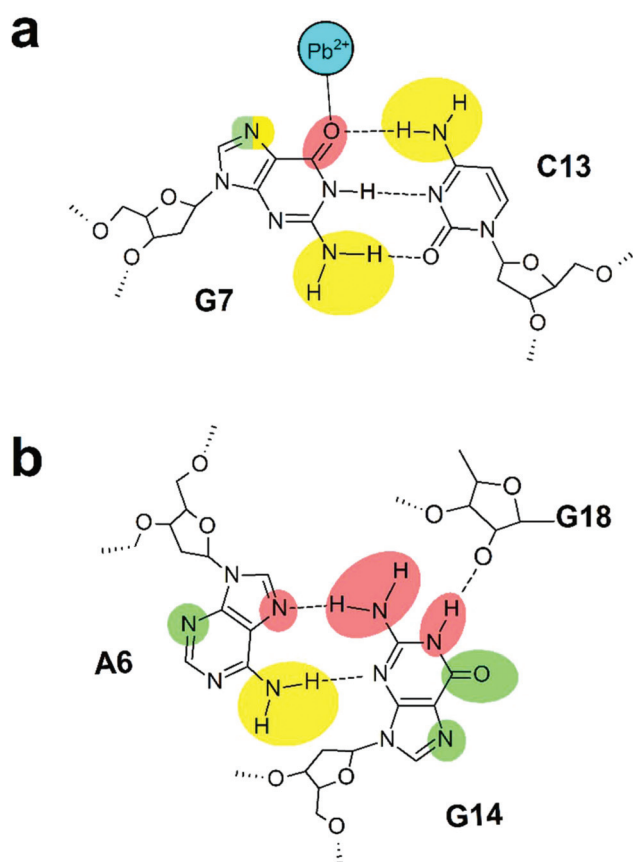


**Fig. 2** Base pairs in the short duplex (P4) observed in the crystal structure of the 8-17 deoxyribozyme and involving residues A6, G7, C13 and G14. Specific groups on the bases are shaded differently depending on the functional impact of their replacement. Green, <10 fold decrease in activity. Yellow, 10- to 100-fold decrease in activity. Red, >100-fold effect on activity. Impacts on activity are from ref. 15, 22, 25, 42 and are summarized in ESI Table 2.† (a) The standard G7-C13 basepair. The G7 base appears rather solvent-accessible in the crystal structure. The substitution of G7 with 7-deazaG yielded less than a threefold decrease in activity in one study<sup>25</sup> but a 5- to 25-fold decrease in another.<sup>22</sup> (b) The noncanonical A6-G14 pair. Hydrogen bonding of the N1 imino group of G14 to the 2'-O group of G18 is also shown (based on the structure obtained with a substrate analog bearing a 2'-O-methyl group at the cleavage site).

The N7 imino groups of G10 and G11 point towards the solvent, which agrees with the functional irrelevance of these groups.<sup>22,25</sup>

(iii) As stated above, G7 and A6 were found to interact with residues 13 and 14 in the bulge loop, forming one regular (G7-C13) and one noncanonical (A6-G14) basepair. This short duplex region (termed P4 by Liu *et al.*<sup>15</sup>) lays perpendicular to the core stem, thus forming a small and compact DNA pseudoknot. While the occurrence of the small P4 duplex had not been predicted, nearly all the groups on A6 and G7 that are involved in this pairing were also important for catalysis (Fig. 2). Additionally, in the structure solved in the presence of lead, the 6-oxo group of the G7 base was forming a direct coordination with a  $\text{Pb}^{2+}$  ion (Fig. 2a).

(iv) As for the "bulge loop" region, the structure placed the G14 base very close to the reaction center, strongly supportive of its role as a general acid-base catalyst, as it will be discussed later. The base was held in place by the nonstandard pairing with A6, part of the AGC loop, as well as by the formation of a standard base pair between nearby C13 and G7. Thus, the strongly conserved A6, G7, C13 and G14 appear to cooperate in the formation of a structural device crucial for activity. A15 also seems to form a nonstandard base pair that, based solely on the structure, might be deemed important: its N9 and hexocyclic amino groups form hydrogen bonds with the G18 base at the cleavage site. This interaction does not fit well with the fact that mutations at positions 15 and 18 are rather well tolerated; for example, replacement of A15 with U only lowered activity by two- to fivefold,<sup>22</sup> whereas the DNAzyme cleaves equally well substrates having a G or A residue at position 18 (at the cleavage site).<sup>17</sup> It is therefore possible that this pair visualized in the crystal structure is not catalytically relevant, or that it can be replaced with different (but perhaps energetically equivalent) interactions in other DNAzyme constructs, in agreement with functional studies.<sup>18</sup> Finally, residues 12 and 15.0 do not form hydrogen bonds with other parts of the complex (consistent with the relatively minor functional effects of mutations at these positions), however T12 stacks on the G7:C13 pair, and lies reasonably close to the metal ion binding site, whereas A15.0 stacks onto the A15-G18 pair.

## The puzzling role of metal ions in folding and catalysis

Even though the original selection procedure that led to the isolation of 8-17 was performed in the presence of  $\text{Mg}^{2+}$ , variants of the same DNAzyme were repeatedly isolated in other *in vitro* selection studies, in which the supplied metal ion cofactors were for example  $\text{Zn}^{2+}$  or  $\text{Cd}^{2+}$ .<sup>11,27</sup> Indeed, a number of detailed studies have established that the 8-17 is activated by an ample and diverse range of divalent metal ions, from  $\text{Ca}^{2+}$  to  $\text{Pb}^{2+}$ .<sup>3,11,16,17,23,42,43</sup> Very high concentrations of  $\text{Na}^+$  or other monovalent cations could also support activity to some extent.<sup>23</sup>

The wide variety of divalent metal ions that can function as cofactors implies a largely unspecific binding of the activating

ions. The titration curves obtained with some of them ( $\text{Mg}^{2+}$ ,  $\text{Ca}^{2+}$ ,  $\text{Mn}^{2+}$ ,  $\text{Zn}^{2+}$  and  $\text{Pb}^{2+}$ ) were essentially monophasic (hyperbolic),<sup>17,42,44</sup> suggesting that a single metal ion is responsible for activation. Overall, the simplest model compatible with these pieces of information is that activity is supported by a single metal ion binding at some low-specificity site.<sup>33,42</sup> Alternative models, in which for example different metal ions bind to distinct (non-overlapping) binding sites and yet manage to activate the reaction seemed unlikely. The single-and-unspecific-site model was somewhat unexpected, considering the abundance of phosphate groups in the DNAzyme structure and hence the high number of potential binding sites for cations.<sup>42</sup>

While the crucial importance of the metal ion for activity was clear, its precise chemical or structural role remained uncertain. One possibility was that the metal ion could be required for structural reasons, *i.e.* for stabilizing a folded and functionally viable structure of the catalyst, as observed with many ribozymes. To address this possibility, the influence of metal ions on the global folding of the 8-17 DNAzyme was extensively explored by fluorescence resonance energy transfer (FRET) on doubly- or triply-labelled constructs.<sup>28,44–46</sup> These studies revealed a complex relationships between metal-promoted DNA folding and activity. The results indicated that a global, metal-dependent DNAzyme folding is not usually observed, and anyway is not required for catalysis, in the presence of  $\text{Pb}^{2+}$ , the metal ion producing the highest activation.<sup>44,45</sup> In contrast, other activating metal ions, such as  $\text{Zn}^{2+}$  and  $\text{Mg}^{2+}$ , were found to induce a global rearrangement, apparently conducive to catalysis.<sup>28,44–46</sup>

These findings led to the conclusion that the 8-17 DNAzyme is structurally pre-organized to accept and catalytically utilize  $\text{Pb}^{2+}$ ;<sup>44,45</sup> this was rather unexpected, given that  $\text{Pb}^{2+}$  had never been used in the selections where the 8-17 motif had been isolated. Another counter-intuitive implication of the FRET studies was that the DNAzyme can perform its reaction within significantly different structural arrangements, depending on the type of available metal ions. However, at the very least, the data with  $\text{Pb}^{2+}$  argued against the possibility that metal ions could play a purely structural role. This conclusion was supported by other pieces of data. In particular, the maximum achievable activity (at saturating metal ion concentrations) varied greatly depending on some chemical–physical properties of the ion type, implying that the metal ions must provide a more direct contribution to the chemical reaction, *e.g.* by changing to different extents the  $\text{pK}_a$  of some reacting group(s).<sup>11,17,42</sup>

In fact, there was a good correlation between the activating ability of different metals (at pH 7.4) and the  $\text{pK}_a$  of the hydrated form of these metals: the lower the  $\text{pK}_a$ , the higher the activation.<sup>42</sup> A similar behavior had been described earlier for the hammerhead ribozyme<sup>47</sup> and a initially interpreted as evidence that a metal-bound hydroxide could act as a general base to deprotonate the reactive 2'-hydroxyl at the cleavage site ( $\gamma$  catalysis).<sup>47</sup> However, now it is well established this functional role is played by conserved G12 (primary

$\gamma$ -catalysis),<sup>48</sup> whereas divalent metal ions may be modulating the reactivity of this base (secondary  $\gamma$ -catalysis)<sup>49</sup> and interact directly with one non-bridging oxygen of the phosphate at the cleavage site (primary  $\beta$ -catalysis).<sup>50</sup> Similarly, in the 8-17 mechanism, different roles of the metal ions could be equally compatible with the observed dependence. For example, a metal bound water molecule, whose acidity would depend on the type of coordinated metal, could serve as a general acid to stabilize the leaving group (secondary  $\delta$  strategy). Generally speaking, it must be noted that the activation efficiencies of different metal ions also show an appreciable correlation with the relative affinities of these ions for oxygen ligands (Fig. S1†) so that the observed dependence of activation on the metal ion type might also be compatible with a direct, catalytic coordination of the metal ion with the leaving group (primary  $\delta$  strategy) or with the non-bridging oxygens at the cleavage site (primary  $\beta$  strategy).

Usually, functional evidence for the interaction of a metal ion with the non-bridging phosphate oxygens is sought by substituting the phosphate linkage with a phosphorothioate, which contains a sulfur atom in place of either the pro-Rp or pro-Sp oxygen. Sometimes, cleavage of one of the two phosphorothioate isomers is substantially hampered when assays are conducted in the presence of 'hard' metal ions such as  $\text{Mg}^{2+}$ , but such a 'thio effect' is attenuated or abolished in the presence of softer, more thiophilic metals such as  $\text{Mn}^{2+}$  or  $\text{Cd}^{2+}$ .<sup>39,51–53</sup> This overall behavior (major thio effect plus rescue by soft metal ions) strongly suggests that the substituted oxygen forms an inner-sphere, catalytic interaction with the metal ion (primary  $\beta$  strategy). Indeed, a few years ago it was reported that 8-17 does not cleave a substrate containing an Rp phosphorothioate at the cleavage site<sup>54</sup> but the study did not report the results of thiophilic metal rescue, so the actual significance of this observation remains uncertain.

In sum, before the appearance of the crystal structure, our understanding of the relationships between metal ions and catalysis of the 8-17 DNAzyme was as follows:

(i) Occupancy of just one divalent metal ion binding site is apparently needed for catalysis.

(ii) This site is strikingly unspecific, being able to accommodate metal ions with different in properties such as size, hardness and coordination preferences.

(iii) The function of the metal ion appears to be purely chemical (direct involvement in catalysis) in the case of  $\text{Pb}^{2+}$ , but could be *also* structural (stabilization of an active conformation) for other metal ions.

(iv) The precise catalytic role of the metal ion in the reaction mechanism remained enigmatic: the available data were similarly compatible with  $\beta$ ,  $\gamma$  or  $\delta$  catalytic strategies (Scheme 1).<sup>55</sup>

## What the crystal structure says about metal ions

As mentioned in the Introduction, only one of the three published 8-17 structures was solved in the presence of divalent

metal ions – as a matter of fact, in the presence of  $\text{Pb}^{2+}$ , the metal ion producing the highest activation. Intriguingly, the crystal structure revealed only one  $\text{Pb}^{2+}$  ion bound in an ordered fashion (albeit with a rather low occupancy of 0.4) to the DNAzyme. The ion is located in a cavity (a metal ion ‘cage’ as defined in the paper) nested between the cleavage site and the center of the catalytic core (Fig. 1a). The inner surface of the ‘cage’ is defined by bases and sugars, but not by phosphate groups. Accordingly, there is no coordination between the metal ion and negatively charged phosphates (a common mode of interaction of metal ions binding to nucleic acids); rather, the  $\text{Pb}^{2+}$  ion showed only one direct coordination to the DNAzyme, with the O6 atom of G7 (Fig. 2a). However, the width of the cage and the distances between  $\text{Pb}^{2+}$  and other heteroatoms of the surrounding residues (mainly within the range of 5–7 Å), suggested that the  $\text{Pb}^{2+}$  bound in this cage could be largely hydrated.<sup>15</sup> While only one metal-coordinated water molecule was observed crystallographically (see below) the presence of other, less ordered water molecules is likely.

The observation of only one metal binding site is in possible agreement with the simple hyperbolic dependence of activity on the concentration of lead.<sup>17</sup> Furthermore, the absence of direct contacts with phosphates and the suggestion that the bound metal ion could retain much of its hydration water molecules, are factors that might help explain the relatively low specificity of the site. As a first approximation, binding sites where cations bind in a largely hydrated form are assumed to be not very selective.<sup>56,57</sup> Another finding that fits nicely with the functional data is the absence of major structural differences in the DNA core when  $\text{Pb}^{2+}$  is bound, consistent with the view that the DNAzyme utilizes lead as a cofactor in a sort of lock-and-key mode, without the need for rearrangements.<sup>44,45</sup>

Previously, the evidence that 8-17 is not active in the presence of  $[\text{Co}(\text{NH}_3)_6]^{3+}$  (frequently used as a probe of outer-sphere interactions for  $[\text{Mg}(\text{H}_2\text{O})_6]^{2+}$ ) had suggested that the catalytic role of the metal ion would not rely on outer-sphere metal coordination, but rather on the direct interaction with some reacting group, for example the internal nucleophile or one non-bridging phosphate oxygen.<sup>23</sup> In the crystal structure, the  $\text{Pb}^{2+}$  ion is far from the position where the internal nucleophile (the 2'-OH of G18) would be; rather, the 2' oxygen appears to interact with the N1 of G14 (Fig. 2b). This argues against a role of the metal ion in activation of the nucleophile, (primary  $\gamma$  strategy). Furthermore, the large distances between  $\text{Pb}^{2+}$  and either the non-bridging  $\text{O}^-$  (5 Å) or the leaving  $\text{O5}'$  (6.9 Å) found in the crystal structure seem inconsistent with a direct binding of the metal ion to these groups. Instead, the crystal structure shows a metal-coordinated water molecule pointing directly towards the leaving group, suggesting a role as a general acid catalyst in the activation of the same group (secondary  $\delta$  strategy,<sup>55</sup> Scheme 1).

The structural and functional evidences for such a role are discussed at length in the following section of this review. In general however it must be borne in mind that the inferences (based on the X-ray structure) about the exact catalytic function

of the metal ion remain somewhat tentative, in particular because it is not sure how close are the available structures to a true pre-catalytic intermediate (see also the Conclusions section).

An obvious limit of the crystallographic study was that it did not solve structures with other metal ions (*i.e.*, different from  $\text{Pb}^{2+}$ ) bound to the DNAzyme. In the peer review file associated to the structural work it is mentioned that crystals cracked when soaked in  $\text{Mg}^{2+}$ .<sup>15</sup> While this experimental observation is potentially consistent with the notion that  $\text{Mg}^{2+}$  induces a conformational change in the DNAzyme,<sup>28,33,44–46</sup> it does not help to understand how different the 8-17 core structure may be in the presence of metal ions other than  $\text{Pb}^{2+}$ . The most parsimonious hypothesis would be that  $\text{Mg}^{2+}$  binds to the same ‘cage’ where  $\text{Pb}^{2+}$  is bound, but with a different binding geometry, imposing a local rearrangement that somehow induces a reorientation of the substrate-binding arms and of the core stem. A distinct possibility (apparently preferred by Liu and coworkers<sup>15</sup>) is that the  $\text{Mg}^{2+}$  ion could bind to a different site on the DNAzyme, inaccessible to lead and responsible for the conformational change.

## Acid–base catalysis in the 8-17 reaction mechanism

Initial studies of the pH-profiles of the 8-17 DNAzyme in presence of  $\text{Zn}^{2+}$ ,  $\text{Mg}^{2+}$ , and  $\text{Pb}^{2+}$  revealed a linear rise of  $\log k_{\text{obs}}$  with increasing pH.<sup>11,17</sup> In all cases the plot showed a slope of  $\sim 1.0$ , suggesting that deprotonation of a single ionizable group is required for catalysis. This group could be the 2'-OH of the nucleotide at the cleavage site, whose deprotonation would help its nucleophilic attack on the adjacent phosphate (Scheme 1). However, the observation of deviation from linearity at pH 8.5 in presence of  $\text{Mg}^{2+}$ ,<sup>42</sup> questioned this idea due to the large difference between the  $\text{pK}_{\text{a}}$  of a 2'-OH and the experimental  $\text{pK}_{\text{a}}$  obtained from the pH-rate profile. Therefore, some other functional group at the catalytic site of the 8-17 DNAzyme should be involved in this process.

In the mechanisms of natural ribozymes, conserved residues often act as general acid–base catalysts. This is the case for the hairpin<sup>58,59</sup> and the hammerhead ribozymes<sup>48,60,61</sup> where a guanine residue (unperturbed  $\text{pK}_{\text{a}} = 9.4$ ) acts as a general base and the same may be true in the mechanisms of the *glmS*,<sup>62</sup> twister,<sup>63,64</sup> pistol<sup>65–68</sup> and Varkud satellite<sup>69,70</sup> ribozymes. In another example, the HDV ribozyme uses a cytosine residue ( $\text{pK}_{\text{a}} = 4.2$ ) as general acid, while the role of a hydrated  $\text{Mg}^{2+}$  as general base is still under discussion.<sup>71,72</sup>

As described above, two guanines and one cytosine residue within the 8-17 catalytic core appeared crucial for activity: G7, G14 and C13.<sup>13,18,22</sup> Could some of these residues be involved in general acid–base catalysis? C13, for example, could act as a general acid in analogy with the case of the HDV ribozyme. However, when the base of C13 was mutated to 5-bromocytosine ( $\text{pK}_{\text{a}} = 2.5$ ), the activity was reduced only fourfold, much less than expected (around 40-fold at neutral pH) considering

the differences in the  $pK_a$  values between C and 5-bromoC.<sup>22</sup> Such a small effect argued against the participation of C13 in proton transfer. In addition, an electron hole migration study identified C13 as having a high solvent accessibility within the DNazyme–substrate complex.<sup>29</sup> As for the two conserved guanines, photo-crosslinking assays indicated that G14 is very proximal to the cleavage site, whereas G7 is somewhat less close.<sup>30</sup> Furthermore, as noted above, mutational and folding studies suggested that the main role of G7 was presumably to stabilize an active conformation of the enzyme.<sup>22,28,29,44,45</sup> On the other hand, G14 seemed a good candidate to act as a general base in the reaction mechanism.

To address this possibility, a recent study analyzed the behavior of three 8-17 variants bearing different G analogues at position 14. Hypoxanthine ( $pK_{a,N1} = 8.7$ ), 2,6-diaminopurine ( $pK_{a,N1} = 5.6$ ) and aminopurine ( $pK_{a,N1} = 3.8$ ) were used for this purpose, so that a broad range of  $pK_a$  values for the N1 imino proton was covered (Fig. 3a).<sup>73</sup> The “standard” 8-17 DNazyme (containing G at position 14) showed a linear pH-rate profile with a slope  $\sim 1.0$ , up to an incipient plateau at pH  $\sim 9$ , consistent with previous observations.<sup>11,17,42</sup> However, the pH-rate profiles of the 8-17 DNazyme variants changed strikingly depending on the  $pK_a$  of the residue in position 14. G14diAP and G14AP, in which the  $pK_a$  of the N1 is considerably decreased, showed a clear plateau in the pH-rate profile above pH 5 (Fig. 3b). Interestingly, the apparent  $pK_a$  values for the pH dependences of the unmodified 8-17 DNazyme and of its G14 variants were in excellent agreement with the  $pK_a$  values of the free bases. These results strongly suggested the participation of the N1 of G14 in a proton transfer event in the mechanism of the 8-17 DNazyme (Fig. 3c).<sup>71</sup>

The simplest possibility to explain this catalytic trend is that G14 acts as a general base in the reaction mechanism. Below the  $pK_a$  of N1, the fraction of deprotonated purine (and hence the efficiency of catalysis) would increase linearly with pH, consistent with the observed pH-activity profiles. At pH  $> pK_{a,N1}$  the base would be largely deprotonated and fully capable of acting as a general base. Consequently, above  $pK_{a,N1}$ , the fraction of the general base would remain constant, providing no further acceleration of the cleavage reaction rate. If G14 is working as a general base, then a general acid with a higher  $pK_a$  value would be required to explain the plateau in the pH-activity plot above  $pK_{a,N1}$ . Accordingly, the increment in reaction rate with pH (up to the plateau) would be associated with the rise in the fraction of deprotonated general base, while the fraction of protonated general acid would remain constant until reaching the group's  $pK_a$ . Beyond the  $pK_a$  of this second group, activity should decrease linearly with the pH.<sup>74</sup> The pH-activity curve expected based on this kinetic model is represented in Fig. 4a.

If G14 acts as a general base, the general acid role might be played by another guanine (or thymine) residue or by an hydrated metal ion, in this case  $Mg^{2+}$  ( $pK_{a,Mg^{2+}} = 11.4$ ).<sup>48,74</sup> The recently published crystal structure of the 8-17 DNazyme, crystallized in presence of  $Pb^{2+}$ , lends support to this latter hypothesis.<sup>15</sup> In fact, although kinetic and crystallization studies used

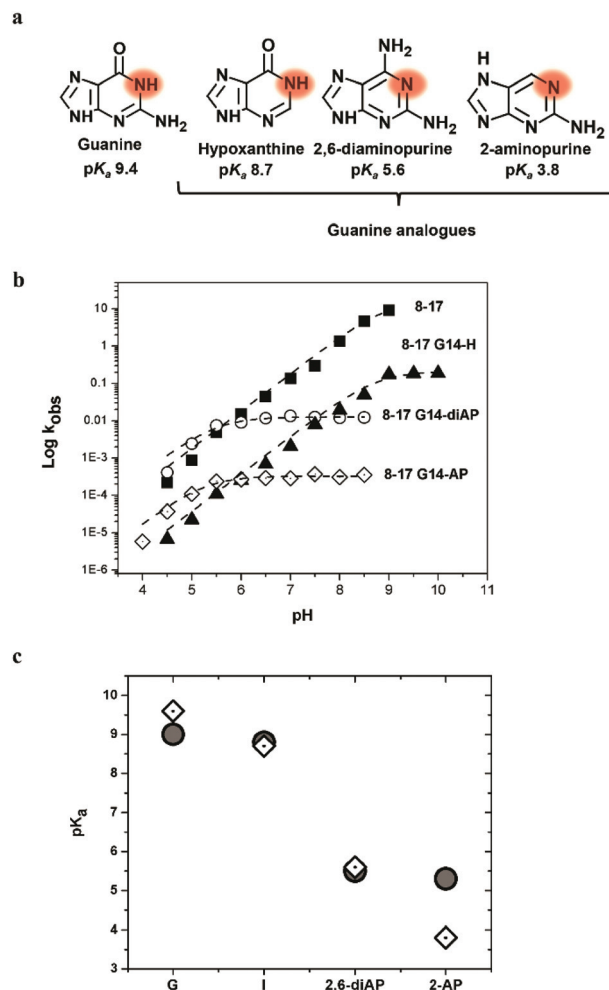


**Fig. 3** (a) Guanine analogues used in this study and the  $pK_a$  of N1 for each of them. (b) Activity of 8-17 and of its variants mutated at G14 as a function of pH. (■) 8-17, (●) 8-17-I (G14-hypoxanthine), (Δ) 8-17-diAP (G14-diaminopurine), (◇) 8-17-AP (G14-aminopurine). The pH-rate profiles were fitted to the equation  $k_{obs} = k_{max}/[1 + 10^{(pK_a - pH)}]$ . (c)  $pK_a$  values of the N1 proton of the 8-17 DNazyme and its variants. White diamonds indicate the  $pK_a$  of free bases and grey circles show the experimental  $pK_a$ , calculated from the pH-rate profiles.<sup>73</sup>

different metal ion cofactors, overall the results suggest similarities in the catalytic strategies regardless of the type of activating metal ion.

## Structure-based current models for the catalytic mechanism of 8-17

The recently solved crystal structures of the 8-17 DNazyme suggest a phosphodiester transesterification that occurs through an in-line attack by the 2'-OH group on the phosphate located at the cleavage site. The non-canonical base pair that G14 forms with A6, induces a conformation that places N1 of G14 3.3 Å from the nucleophile O2' (in the structure where a 2'-O-methyl nucleotide was present at the cleavage site: see Fig. 2b). This proximity would allow the deprotonated G14 to



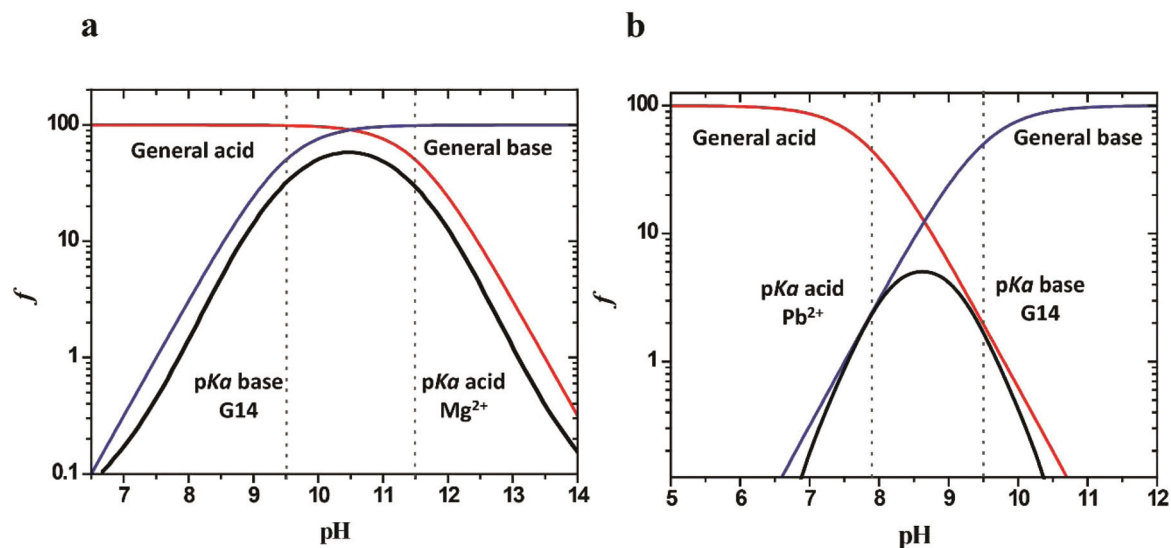


**Fig. 4** Simulation of the fraction of the general base (blue traces) and general acid (red traces) as a function of pH. The plots explain the kinetic models for general acid–base catalysis, considering (a) G14 as general base and hydrated Mg<sup>2+</sup> as general acid and (b) G14 as general base and hydrated Pb<sup>2+</sup> as general acid. Black curves show the predicted activity profile according to the proposed kinetic model. Both plots help to describe the influence of pH on the 8-17 DNAzyme activity.

act as a general base, to remove the proton from the 2'-OH and increase the nucleophilicity of this reacting group (primary  $\gamma$ -catalysis). On the other hand, O6 from G7 is the only atom directly coordinated to the Pb<sup>2+</sup> ion (2.9 Å), according to the crystallographic information. At the same time, Pb<sup>2+</sup> is coordinated to a water molecule. No other (ordered) water molecules were observed at the active site. Coordination to the metal ion is expected to decrease the pK<sub>a</sub> of the water molecule, facilitating its role as general acid, possibly stabilizing the O5' leaving group (secondary  $\delta$ -catalysis).<sup>15</sup> Liu and co-workers elaborated these concepts into a first, hypothetical mechanism of the 8-17 reaction, illustrated in Fig. 5a.<sup>15</sup>

If the catalytic strategies in Fig. 5a are part of the reaction mechanism of the 8-17 DNAzyme, then the kinetic model should agree with the observed pH dependence of the DNAzyme activity, measured in the presence of different metal ions. If a water molecule coordinated to Mg<sup>2+</sup> acts as a general acid, to stabilize the O5' leaving group, its fraction would remain constant at pH < pK<sub>a</sub> value (11.4, if we equate its pK<sub>a</sub> to the pK<sub>a</sub> of hydrated Mg<sup>2+</sup>). This would explain the plateau region observed above the pK<sub>a</sub> value of the purine in position 14 (Fig. 3b). This model is summarized in Fig. 4a. Experimentally, it is not possible to carry out measurements above the pK<sub>a</sub> of the general acid to test the expected drop in the reaction rate. Following the same analysis, in the presence of Pb<sup>2+</sup> the pH-rate profile of the 8-17 DNAzyme should exhibit the same trend, although the plateauing region should be expected around pH 8 (pK<sub>a,Pb<sup>2+</sup></sub> = 7.8). In this case a linear drop in the activity should occur above pH 9, the experimental pK<sub>a</sub> of G14 (Fig. 4b). Even though in the case of Pb<sup>2+</sup>, the pK<sub>a</sub> value is much lower than Mg<sup>2+</sup>, the high efficiency of the enzyme in presence of this metal ion at high pH has made it

difficult to measure of the reaction rate manually under such conditions.

The available crystal structures also offered the possibility to develop theoretical models to draw details into its reaction mechanism. Recent molecular dynamics simulations performed by York and coworkers,<sup>75,76</sup> provided mimics for crucial states in the reaction pathway that gave valuable insights into the possible catalytic strategies employed by the 8-17. These theoretical studies suggest that Pb<sup>2+</sup> in the transition state could be directly coordinating to the non-bridging phosphate oxygen and the O5' leaving group. Through this inner-sphere coordination, Pb<sup>2+</sup> would be participating to different types of catalytic strategies, providing stabilization of the dianionic transition state (primary  $\beta$ -catalysis) as well as stabilization of the leaving group as a Lewis acid (primary  $\delta$ -catalysis).<sup>75</sup> In such an arrangement, the metal would further help to remove the non-productive hydrogen bonding of the nucleophile to the non-bridging phosphate oxygen (tertiary  $\gamma$ -catalysis).<sup>76</sup> Overall, the results of these simulations offer an alternative plausible mechanisms of catalysis, although they do not completely rule out the possibility of a Pb<sup>2+</sup>-bound water acting as a general acid (secondary  $\delta$ -catalysis). The supplementary materials of the same study present preliminary simulations of the transition state using Mg<sup>2+</sup> as a cofactor. Two binding modes are projected for Mg<sup>2+</sup>. In both, the metal ion is directly coordinated to the non-bridging oxygen and to a water molecule that stabilizes the O5' leaving group. The main difference between the two representations is that in one, Mg<sup>2+</sup> is coordinated to the O6 of G7, while in the other there is no such an interaction. To probe the catalytic model with G14 acting as general base and a water molecule coordinated to the metal ion acting as a

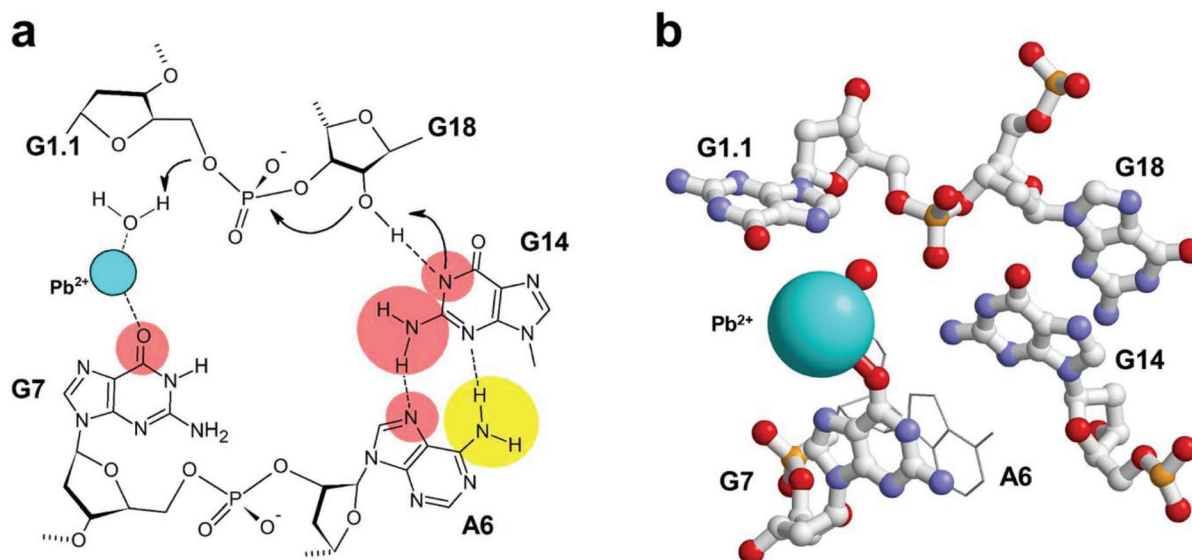


**Fig. 5** (a) Possible mechanism for the 8-17 DNAzyme reaction, proposed by Liu *et al.* based on the available crystal structures.<sup>15</sup> The scheme illustrates the non-standard base pair between A6 and G14 that places N1 of G14 close to the 2'-OH group at the cleavage site. The scheme also shows the water molecule coordinated to  $\text{Pb}^{2+}$  and the interaction of the same ion with O6 from G7.<sup>15</sup> Red and yellow circles display the functional relevance of specific base groups on the activity of 8-17 according to the scale described in the legend of Fig. 2. (b) A close-up of the 8-17 core structure (PDB: 5XM8) helps appreciate the actual three-dimensional dislocation of the same residues shown schematically in panel a. The A6 base (represented as wireframe, for clarity) is stacking onto G7, in addition to being hydrogen bonded to G14. The  $\text{Pb}^{2+}$  ion, but not its coordinated water molecule, is shown as its van der Waals surface. The 2'-OH at the cleavage site is not present because G18 is a deoxyribonucleotide in the substrate analog used for crystallization.

general acid (primary  $\gamma$ -catalysis and secondary  $\delta$ -catalysis, respectively), as shown in the mechanism proposed in Fig. 5a, it would be necessary to have crystal structures of the active conformation of 8-17 in presence of other metal ions such as  $\text{Mg}^{2+}$  or  $\text{Zn}^{2+}$ , in addition to pH-rate profiles measured using other metal ions as cofactors. These latter data might provide robust evidence about the  $\text{pK}_a$  of the water molecule coordinated to metal ions other than  $\text{Pb}^{2+}$ .

In ribozyme catalysis, it has been proposed that charged nucleobases or metal ions in the active site can provide cooperative interactions to shift the  $\text{pK}_a$  of the general bases or general acids to improve their ability as catalysts.<sup>77</sup> For the hammerhead ribozyme, it has been proposed that a cationic cytosine or a  $\text{Mg}^{2+}$  ion could be assisting the shift of the  $\text{pK}_a$  of the general base guanine.<sup>60,78</sup> However the crystal structure of the 8-17 places G14 distant from the  $\text{Pb}^{2+}$  ion (Fig. 5b), so that no such cooperative interactions of the base with this metal ion should be expected.<sup>15</sup> Nevertheless, theoretical models of some key states of the reaction pathway have suggested the participation of  $\text{Na}^+$  in different catalytic strategies in the mechanism of reaction of the 8-17.<sup>75</sup> In one of these states,  $\text{Na}^+$  is interacting with the Hoogsteen edge of G14 when this base is deprotonated. The authors of this study have suggested that this interaction would help to increase the acidity of the purine in position 14, through a secondary  $\gamma$ -catalysis strategy.<sup>75</sup> Thus the coincidence of kinetic  $\text{pK}_a$  values and free base  $\text{pK}_a$  values, shown in Fig. 3c, would be the result of two balancing effects: the effect of an electronegative environment,

which tends to raise the  $\text{pK}_a$  of the purine in position 14; and the effect of interacting  $\text{Na}^+$ , that works in the opposite sense. This balancing of electrostatic effects in modulating the acidity of nucleobases may be a recurring mechanism in catalytic nucleic acids.<sup>60,78</sup> To better explore the contribution of monovalent cations to this and other catalytic strategies used by the 8-17 (envisaged the same computational study<sup>75</sup>), it may be worth conducting kinetic experiments (*e.g.*, divalent metal titrations) using buffers devoid of  $\text{Na}^+$  and containing very different monovalent cations such as tetramethylammonium.

Additionally, very recent theoretical studies have suggested the existence of a common structural platform shared by several ribozymes and the 8-17 DNAzyme. Authors have named this functional architecture the L-scaffold, which is formed by two key elements: the L-anchor and the L-pocket.<sup>79</sup> The anchor serves to position the conserved guanine that acts as general base close to the 2'-OH nucleophile and the L-pocket facilitates the formation of the divalent metal ion binding site. In the 8-17, A6 performs the anchoring role by pairing G14 (Fig. 2b) supporting a tertiary  $\gamma$  catalysis, meanwhile G7 forms part of the L-pocket that facilitate the binding of the divalent metal through a tertiary  $\delta$  catalytic strategy.<sup>79</sup> While the crystal structure shows  $\text{Pb}^{2+}$  bound to O6 from G7,<sup>15</sup> simulations suggest an alternative possible binding mode involves  $\text{Pb}^{2+}$  directly coordinated to the non-bridging phosphate oxygen and indirectly coordinated to the Hoogsteen edge of G7.<sup>79</sup>

As mentioned above, it is known that the overall conformation of the 8-17 DNAzyme does not change in the presence

of  $\text{Pb}^{2+}$  (and in fact no changes were observed in the crystal structure with  $\text{Pb}^{2+}$  bound) but does change in presence of  $\text{Mg}^{2+}$ . Despite this, earlier observations have demonstrated the importance of the same bases and even the same functional groups for catalysis in the presence of different metal ions. For example, the crucial role of O6 from the highly conserved G7 was revealed after observing a  $10^4$ -fold drop in the activity of the enzyme when the guanine residue was replaced by a 6-thioguanine analogue. The drop was observed in the presence of 3 mM  $\text{Mg}^{2+}$ , but similar results were found in the presence of  $\text{Ca}^{2+}$  or  $\text{Mn}^{2+}$  (ESI Table 2†).<sup>22</sup> In the crystal structure study, Liu and coworkers also showed the importance of O6 from G7, by measuring the activity of a modified enzyme with a 6-OMe guanine analogue at position 7 in presence of  $\text{Pb}^{2+}$ . The reaction rate constant was  $\sim 30$  times lower for the mutant (ESI Table 2†). These observations raise significant questions. For example, can really the DNzyme, in the presence of different metal ions, employ the same bases and groups to catalyze RNA-cleavage, despite differences in overall folding? And, more generally, how do the 8-17 catalytic strategies relate to the metal ion promiscuity exhibited by the enzyme? Certainly, more research is needed to answer these questions.

## Conclusions

Today it is accepted that DNA can catalyze many chemical reactions (see ref. 6 and 80 for recent reviews) and that it can do this with an efficiency comparable to that of the naturally evolved protein enzymes and ribozymes, despite its poorer assortment of functional groups.<sup>6,81</sup> However, our knowledge of the structural and mechanistic basis of DNA catalysis remains particularly modest. For example, high-resolution structural data on DNzymes are very scarce. Furthermore, while a reasonable expectation was that DNzymes in general would share with their ribozyme counterparts common contributions to catalysis, such as acid-base chemistry involving the nucleobases,<sup>6</sup> positive proofs have been limited.<sup>82</sup>

Related to this general issue, the recently obtained 8-17 crystal structures, combined and contrasted with the body of functional data available on the same DNzyme, offer excellent and perhaps unique prospects for understanding the detailed mechanisms by which a DNA enzyme catalyzes its reaction. As we have discussed, the features of the crystal structure, while sometimes unpredicted, are in remarkable agreement with the results of earlier functional studies.<sup>15</sup> This observation has several implications. First, it suggests that the structure reflects a catalytically active conformer of 8-17. Second, it supports the use of the features observed in the structure to interpret the mechanism of the DNzyme. Third, it suggests new experimental approaches to test those aspects of mechanism that the structure does not fully explain or help to clarify.

In particular, the combination of functional and structural data has provided a first reasonably complete model for the catalytic mechanism of 8-17.<sup>15</sup> The model (Fig. 5a) postulates that 8-17 employs an  $\alpha$ -catalytic strategy (by achieving an in-

line alignment of the reacting groups), primary  $\gamma$ -strategy (mediated by G14 acting as a general base) and secondary  $\delta$ -catalysis (operated by a metal bound water molecule, acting as a general acid). This model should not be considered final, but represents a point of reference for further research in the field. For example, recent computational studies from the York group have offered the opportunity to test this proposed mechanism and also other plausible mechanism have emerged.<sup>75,76,79</sup>

Indeed, while the model proposed in the structural paper is broadly in agreement with most of the functional data, many of its details remain hypothetical and need to be tested and validated by further studies. Most fundamentally, this need arises because it is debatable how close are the available structures to a true pre-catalytic intermediate. Arguably, a structure of the DNzyme bound to a substrate with a 2'-O-methyl group at the cleavage site, in the presence of  $\text{Pb}^{2+}$ , could represent most closely such a pre-catalytic species, but this kind of a structure was not obtained. Hence, as pointed out by one of the referees of the structural paper,<sup>15</sup> the current mechanistic model, albeit attractive, represents a combination of information from three structures, none of which individually corresponds to a pre-catalytic state intermediate. Far from devaluing the pivotal importance of the crystallographic analyses by Liu *et al.*, this stresses the need for additional experiments to address the suggestions arising from the available structures.

One specific issue that the structures do not clarify beyond any reasonable doubt, is the exact role of the metal ion in catalysis. The model associates the metal ion to a secondary  $\delta$ -catalytic strategy and excludes primary  $\beta$ -catalysis, but phosphorothioate experiments provide suggestions for some (catalytically important) interaction of the non-bridging pro-Rp oxygen at the cleavage site.<sup>54</sup> As mentioned earlier, dynamical simulations suggested the possibility of direct interaction of the metal with the pro-Rp oxygen in four key states along the reaction pathway (primary  $\beta$ -catalysis).<sup>75,76,79</sup> Thus, could the metal ion (in the transition state, or immediately prior to it) be coordinating to the pro-Rp oxygen? Or perhaps, could it be donating a proton to the same oxygen through a coordinated water molecule? More thorough studies with a phosphorothioate at the cleavage site might presumably help to understand whether the metal ion is involved in a catalytically relevant interaction with the non-bridging oxygen(s).

Furthermore, the crystal structures provide some suggestions but no direct insight into the features that allow the 8-17 DNzyme to 'promiscuously' employ different types of metal ions (associated with different folding patterns). How does the binding mode change for ions that differ greatly in terms of ionic radius and preferred coordination geometry? What is the conformational change induced by binding of metal ions other than  $\text{Pb}^{2+}$ ? And, is the mechanism the same regardless of the metal ion? Addressing these questions entails the execution of further structural studies.

There are other fascinating questions associated to the 8-17 function that the crystal structures do not help to address. One

example regards the cleavage site selectivity. As noted above, A15 in the crystal structure forms two hydrogen bonds with the G18 base at the cleavage site, but it is not clear how this may contribute to specificity, since substrates with different nucleotides at position 18 can be cleaved with substantial efficiency.<sup>17,18</sup> Also, while the G1.1-T2.1 wobble pair seems important for function, the precise reasons remain to be proven. Schlosser *et al.* several years ago identified 8-17 variants that could cleave efficiently substrates containing A or C at position 1.1.<sup>18</sup> However, the sequences of those variants differed significantly from the sequence used in the crystallographic study – in particular, the Schlosser variants apparently lacked a residue in position 2.1 – so it is not clear how the available structural data can help interpret these earlier findings.

Similarly, it is well known that the DNAzyme cleaves less efficiently an all-RNA substrate, as compared to one in which only the residue 18 is a ribonucleotide.<sup>11,16</sup> This feature might be connected with the type of helices formed in the DNAzyme-substrate complex (A-type *versus* B-type) and possibly on their effect on the alignment of reacting groups ( $\alpha$ -strategy, Scheme 1), but since all the substrate analogs used in the crystal study were mostly DNA, this remains an educated guess. Finally, the structures do not explain why the reaction of 8-17 (in the presence of  $Mg^{2+}$  at least) is virtually irreversible<sup>83</sup> in contrast to what is observed with some ribozymes (such as the hairpin ribozyme) that catalyze exactly the same transesterification process. Possibly, attainment of a crystal structure of the DNAzyme complexed to its products would provide valuable information on this topic.

## Conflicts of interest

There are no conflict to declare.

## Acknowledgements

This material is based upon work supported by Fondecyt Regular 1181438 and also has benefited from the framework of the COMP-HUB Initiative, funded by the ‘Departments of Excellence’ program of the Italian Ministry for Education, University and Research (MIUR, 2018–2022).

## References

- 1 R. R. Breaker and G. F. Joyce, *Chem. Biol.*, 1994, **1**, 223–229.
- 2 S. W. Santoro and G. F. Joyce, *Biochemistry*, 1998, **37**, 13330–13342.
- 3 S. W. Santoro and G. F. Joyce, *Proc. Natl. Acad. Sci. U. S. A.*, 1997, **94**, 4262–4266.
- 4 H. E. Ihms and Y. Lu, in *Ribozymes: Methods and Protocols*, ed. J. S. Hartig, Humana Press, Totowa, NJ, 2012, pp. 297–316, DOI: 10.1007/978-1-61779-545-9\_18.
- 5 S. K. Silverman, *Nucleic Acids Res.*, 2005, **33**, 6151–6163.
- 6 S. K. Silverman, *Trends Biochem. Sci.*, 2016, **41**, 595–609.
- 7 W. Zhou, R. Saran and J. Liu, *Chem. Rev.*, 2017, **117**, 8272–8325.
- 8 K. Hwang, Q. Mou, R. J. Lake, M. Xiong, B. Holland and Y. Lu, *Inorg. Chem.*, 2019, **58**(20), 13696–13708.
- 9 H. Wang, Y. Chen, H. Wang, X. Liu, X. Zhou and F. Wang, *Angew. Chem.*, 2019, **131**, 7458–7462.
- 10 J. Feng, Z. Xu, F. Liu, Y. Zhao, W. Yu, M. Pan, F. Wang and X. Liu, *ACS Nano*, 2018, **12**, 12888–12901.
- 11 J. Li, W. Zheng, A. H. Kwon and Y. Lu, *Nucleic Acids Res.*, 2000, **28**, 481–488.
- 12 D. Faulhammer and M. Famulok, *J. Mol. Biol.*, 1997, **269**, 188–202.
- 13 R. P. G. Cruz, J. B. Withers and Y. Li, *Chem. Biol.*, 2004, **11**, 57–67.
- 14 K. Schlosser and Y. Li, *ChemBioChem*, 2010, **11**, 866–879.
- 15 H. Liu, X. Yu, Y. Chen, J. Zhang, B. Wu, L. Zheng, P. Haruehanroengra, R. Wang, S. Li, J. Lin, J. Li, J. Sheng, Z. Huang, J. Ma and J. Gan, *Nat. Commun.*, 2017, **8**, 2006.
- 16 A. Peracchi, *J. Biol. Chem.*, 2000, **275**, 11693–11697.
- 17 A. K. Brown, J. Li, C. M. B. Pavot and Y. Lu, *Biochemistry*, 2003, **42**, 7152–7161.
- 18 K. Schlosser, J. Gu, L. Sule and Y. Li, *Nucleic Acids Res.*, 2008, **36**, 1472–1481.
- 19 R. R. Breaker, G. M. Emilsson, D. Lazarev, S. Nakamura, I. J. Puskarz, A. Roth and N. Sudarsan, *RNA*, 2003, **9**, 949–957.
- 20 Y. Li and R. R. Breaker, *J. Am. Chem. Soc.*, 1999, **121**, 5364–5372.
- 21 P. C. Bevilacqua, M. E. Harris, J. A. Piccirilli, C. Gaines, A. Ganguly, K. Kostenbader, S. Ekesan and D. M. York, *ACS Chem. Biol.*, 2019, **14**, 1068–1076.
- 22 A. Peracchi, M. Bonaccio and M. Clerici, *J. Mol. Biol.*, 2005, **352**, 783–794.
- 23 D. Mazumdar, N. Nagraj, H.-K. Kim, X. Meng, A. K. Brown, Q. Sun, W. Li and Y. Lu, *J. Am. Chem. Soc.*, 2009, **131**, 5506–5515.
- 24 B. Wang, L. Cao, W. Chiuman, Y. Li and Z. Xi, *Biochemistry*, 2010, **49**, 7553–7562.
- 25 W. Rong, L. Xu, Y. Liu, J. Yu, Y. Zhou, K. Liu and J. He, *Bioorg. Med. Chem. Lett.*, 2012, **22**, 4238–4241.
- 26 S. Donini, M. Clerici, J. Wengel, B. Vester and A. Peracchi, *J. Biol. Chem.*, 2007, **282**, 35510–35518.
- 27 A. Kasproicz, K. Stokowa-Soltys, J. Wrzesinski, M. Jezowska-Bojczuk and J. Ciesiolka, *Dalton Trans.*, 2015, **44**, 8138–8149.
- 28 N. K. Lee, H. R. Koh, K. Y. Han and S. K. Kim, *J. Am. Chem. Soc.*, 2007, **129**, 15526–15534.
- 29 E. K. Y. Leung and D. Sen, *Chem. Biol.*, 2007, **14**, 41–51.
- 30 Y. Liu and D. Sen, *J. Mol. Biol.*, 2008, **381**, 845–859.
- 31 W. Zhou, Y. Zhang, J. Ding and J. Liu, *ACS Sens.*, 2016, **1**, 600–606.
- 32 S. Du, Y. Li, Z. Chai, W. Shi and J. He, *Bioorg. Chem.*, 2019, 103401.
- 33 A. Peracchi, M. Bonaccio and A. Credali, *Org. Biomol. Chem.*, 2017, **15**, 8802–8809.



- 34 J. Nowakowski, P. J. Shim, G. S. Prasad, C. D. Stout and G. F. Joyce, *Nat. Struct. Biol.*, 1999, **6**, 151–156.
- 35 H. W. Pley, K. M. Flaherty and D. B. McKay, *Nature*, 1994, **372**, 68–74.
- 36 W. G. Scott, J. T. Finch and A. Klug, *Cell*, 1995, **81**, 991–1002.
- 37 D. McKay, *RNA*, 1996, **2**, 395–403.
- 38 A. Peracchi, J. Matulic-Adamic, S. Wang, L. Beigelman and D. Herschlag, *RNA*, 1998, **4**, 1332–1346.
- 39 S. Wang, K. Karbstein, A. Peracchi, L. Beigelman and D. Herschlag, *Biochemistry*, 1999, **38**, 14363–14378.
- 40 M. Martick and W. G. Scott, *Cell*, 2006, **126**, 309–320.
- 41 J. A. Nelson and O. C. Uhlenbeck, *RNA*, 2008, **14**, 605–615.
- 42 M. Bonaccio, A. Credali and A. Peracchi, *Nucleic Acids Res.*, 2004, **32**, 916–925.
- 43 W. J. Moon and J. Liu, *ChemBioChem*, 2019, DOI: 10.1002/cbic.201900344.
- 44 H.-K. Kim, J. Liu, J. Li, N. Nagraj, M. Li, C. M. B. Pavot and Y. Lu, *J. Am. Chem. Soc.*, 2007, **129**, 6896–6902.
- 45 H.-K. Kim, I. Rasnik, J. Liu, T. Ha and Y. Lu, *Nat. Chem. Biol.*, 2007, **3**, 763.
- 46 J. C. Lam and Y. Li, *ChemBioChem*, 2010, **11**, 1710–1719.
- 47 S. C. Dahm, W. B. Derrick and O. C. Uhlenbeck, *Biochemistry*, 1993, **32**, 13040–13045.
- 48 J. Han and J. M. Burke, *Biochemistry*, 2005, **44**, 7864–7870.
- 49 M. Roychowdhury-Saha and D. H. Burke, *RNA*, 2006, **12**, 1846–1852.
- 50 W. L. Ward and V. J. DeRose, *RNA*, 2012, **18**, 16–23.
- 51 P. Thaplyal, A. Ganguly, B. L. Golden, S. Hammes-Schiffer and P. C. Bevilacqua, *Biochemistry*, 2013, **52**, 6499–6514.
- 52 J. M. Warnecke, J. P. Furste, W. D. Hardt, V. A. Erdmann and R. K. Hartmann, *Proc. Natl. Acad. Sci. U. S. A.*, 1996, **93**, 8924–8928.
- 53 J. K. Frederiksen and J. A. Piccirilli, *Methods*, 2009, **49**, 148–166.
- 54 P. J. Huang and J. Liu, *Nucleic Acids Res.*, 2015, **43**, 6125–6133.
- 55 G. M. Emilsson, S. Nakamura, A. Roth and R. R. Breaker, *RNA*, 2003, **9**, 907–918.
- 56 T. Dudev and C. Lim, *J. Phys. Chem. B*, 2001, **105**, 4446–4452.
- 57 G. Eisenman and J. A. Dani, *Annu. Rev. Biophys. Biophys. Chem.*, 1987, **16**, 205–226.
- 58 R. Pinard, K. J. Hampel, J. E. Heckman, D. Lambert, P. A. Chan, F. Major and J. M. Burke, *EMBO J.*, 2001, **20**, 6434–6442.
- 59 S. Kath-Schorr, T. J. Wilson, N.-S. Li, J. Lu, J. A. Piccirilli and D. M. J. Lilley, *J. Am. Chem. Soc.*, 2012, **134**, 16717–16724.
- 60 E. A. Frankel, C. A. Strulson, C. D. Keating and P. C. Bevilacqua, *Biochemistry*, 2017, **56**, 2537–2548.
- 61 T.-S. Lee, C. S. López, G. M. Giambaşu, M. Martick, W. G. Scott and D. M. York, *J. Am. Chem. Soc.*, 2008, **130**, 3053–3064.
- 62 D. J. Klein, M. D. Been and A. R. Ferré-D'Amaré, *J. Am. Chem. Soc.*, 2007, **129**, 14858–14859.
- 63 T. J. Wilson, Y. Liu, C. Domnick, S. Kath-Schorr and D. M. J. Lilley, *J. Am. Chem. Soc.*, 2016, **138**, 6151–6162.
- 64 D. Eiler, J. Wang and T. A. Steitz, *Proc. Natl. Acad. Sci. U. S. A.*, 2014, **111**, 13028–13033.
- 65 K. A. Harris, C. E. Lünse, S. Li, K. I. Brewer and R. R. Breaker, *RNA*, 2015, **21**, 1852–1858.
- 66 A. Ren, N. Vušurović, J. Gebetsberger, P. Gao, M. Juen, C. Kreutz, R. Micura and D. J. Patel, *Nat. Chem. Biol.*, 2016, **12**, 702.
- 67 T. J. Wilson, Y. Liu, N.-S. Li, Q. Dai, J. A. Piccirilli and D. M. J. Lilley, *J. Am. Chem. Soc.*, 2019, **141**, 7865–7875.
- 68 L. A. Nguyen, J. Wang and T. A. Steitz, *Proc. Natl. Acad. Sci. U. S. A.*, 2017, **114**, 1021–1026.
- 69 T. J. Wilson, A. C. McLeod and D. M. J. Lilley, *EMBO J.*, 2007, **26**, 2489–2500.
- 70 M. D. Smith, R. Mehdizadeh, J. E. Olive and R. A. Collins, *RNA*, 2008, **14**, 1942–1949.
- 71 S.-i. Nakano, D. M. Chadalavada and P. C. Bevilacqua, *Science*, 2000, **287**, 1493–1497.
- 72 S. R. Das and J. A. Piccirilli, *Nat. Chem. Biol.*, 2005, **1**, 45–52.
- 73 M. Cepeda-Plaza, C. E. McGhee and Y. Lu, *Biochemistry*, 2018, **57**, 1517–1522.
- 74 P. C. Bevilacqua, *Biochemistry*, 2003, **42**, 2259–2265.
- 75 Ş. Ekesan and D. M. York, *Nucleic Acids Res.*, 2019, **47**, 10282–10295.
- 76 A. Ganguly, B. P. Weissman, J. A. Piccirilli and D. M. York, *ACS Catal.*, 2019, **9**, 10612–10617.
- 77 E. A. Frankel and P. C. Bevilacqua, *Biochemistry*, 2018, **57**, 483–488.
- 78 H. Chen, T. J. Giese, B. L. Golden and D. M. York, *Biochemistry*, 2017, **56**, 2985–2994.
- 79 C. S. Gaines, J. A. Piccirilli and D. M. York, *RNA*, 2020, **26**(2), 111–125.
- 80 M. Hollenstein, *Molecules*, 2015, **20**, 20777–20804.
- 81 A. Peracchi, *ChemBioChem*, 2005, **6**, 1316–1322.
- 82 L. Ma, S. Kartik, B. Liu and J. Liu, *Nucleic Acids Res.*, 2019, **47**, 8154–8162.
- 83 A. Flynn-Charlebois, T. K. Prior, K. A. Hoadley and S. K. Silverman, *J. Am. Chem. Soc.*, 2003, **125**, 5346–5350.